Cellulose (2025) 32:1979–1991
https://doi.org/10.1007/s10570-024-06365-y

ORIGINAL RESEARCH

Design and fabrication of mesh-like four-warp leno cotton fabric based on self-locking effect: outstanding mechanical performance and breathability

Xiao Tian · Meiyu Yao · Ying Li · Li Li

Received: 31 July 2024 / Accepted: 28 December 2024 / Published online: 4 January 2025

Abstract Achieving a fabric with good mechanical performance and breathability is significant for the development of protective clothing. The leno structure is a desirable fabric design for enhancing these properties due to its advantageous characteristics, such as flexibility, lightness, diamond-shaped structure, and increased yarn interlacing. However, there is a lack of studies focused on developing novel leno structures because of the difficulty of weaving and exploring the mechanical behavior and breathability of various leno fabrics with different structural characteristics. In this study, we leveraged advanced weaving techniques with improved needle-shaped heald frames to develop a programmed mesh-like four-warp leno cotton fabric that offers outstanding mechanical performance and breathability. The efficacy of the self-locking effects, achieved by manipulating the yarn interweaving to simultaneously regulate yarn friction and fabric porosity, is experimentally demonstrated. Compared to plain structures of the same density, the four-warp leno (FL) fabric exhibits nearly twice the tensile strength and strain in the warp direction. Additionally, the four-warp leno fabric demonstrates greater displacements to reach the junction rupture force point than plain structure of the same density in the yarn pull out tests, owing to the self-locked interweaving of the warp yarns. The yarn pull-out behavior of the FL was analyzed to illustrate the variation in load and displacement. Moreover, the high porosity of the four-warp leno woven fabric results in excellent air permeability, thermal conductivity, and water vapor transmission. This study provides an effective strategy for designing and fabricating four-warp leno fabric with outstanding mechanical performance and breathability for diverse applications.

Keywords Four-warp leno · Self-locking effect · Mechanical performance · Breathability · Yarn pull-out behavior

X. Tian · M. Yao · Y. Li
School of Fashion and Textiles, The Hong Kong Polytechnic University, Hung Hom, Kowloon, Hong Kong 999077, China

L. Li (✉)
The Division of Integrative Systems and Design, The Hong Kong University of Science and Technology, Clear Water Bay, Kowloon, Hong Kong 999077, China
e-mail: lillyli@ust.hk

Introduction

The mechanical properties and breathable characteristics of textiles are important factors to consider when designing and fabricating functional textiles, such as protective clothing (Zhao et al. 2023). Protective clothing not only facilitates the rapid expulsion of heat and moisture to maintain the wearer's comfort but also requires good mechanical strength and abrasion resistance, especially in demanding work environments like fire incidents and emergency

rescue situations (Houshyar et al. 2017; Pamuk et al. 2023; Schwarz et al. 2020). Therefore, it is essential to explore fabrics that can enhance mechanical properties without compromising breathability (Kalazić et al. 2022; Tan et al. 2024; Iftikhar et al. 2020).

Textile structures play a critical role in controlling the mechanical properties of materials (Sanchez et al. 2021; Jahan 2017; Limeneh et al. 2022). Woven structures are ideal due to their stability and higher strength compared to knitted and non-woven fabric structures. Developing woven structures can thus effectively address the issue of low mechanical properties. In recent years, various woven fabrics, such as graphene-modified woven fabric (Bhattacharjee et al. 2019), shear-thickening fluid-enhanced woven fabric (Gong et al. 2014; Qiu et al. 2023), and softener and wetting agent-treated woven fabric (Tang et al. 2017), have demonstrated superior mechanical performance. However, breathability is often compromised by the impact of functional treatment agents in the fabric, which limits comfort. Additionally, the finishing agents used to enhance mechanical properties may contribute to environmental pollution.

To address these limitations, special structural design is considered an effective strategy for improving both mechanical performance and breathability. The leno woven structure is an ideal fabric design that enhances both properties by having two warp yarns cross each other and interlace with the weft yarn through a twisting action, which helps hold the weft yarn in place (Weise et al. 2019; Saha et al. 2017). Previous studies have shown that incorporating leno lines into a plain weave structure can increase the junction rupture force (Yi et al. 2019), and fabrics with leno weave structures can improve gripping efficiency (Zhou et al. 2014), energy absorption under high impact loads, and the reinforcing efficiency between textiles and concrete (Zhang et al. 2020; Lenz et al. 2015). Furthermore, the strong interlocking structure of leno fabric creates a fabric with an open or lace-like appearance similar to regular gauze (Shaker et al. 2020), allowing light and air to easily pass through. Despite its many advantages, leno woven fabric has limitations in structural stability due to yarn crossing, which necessitates improvements through structural variations. Moreover, there is a lack of studies focused on developing novel leno structures due to weaving difficulties. Additionally, limited research has explored the mechanical behavior and breathability of various leno fabrics with different structural characteristics. Therefore, there is a significant demand for developing a novel leno woven fabric that enhances both breathability and mechanical performance through sustainable fabrication methods.

In this work, we developed a novel four-warp leno woven fabric (FL) with excellent mechanical properties and breathability using advanced weaving techniques with improved needle-shaped heald frames. The four warp threads intersect and interweave with the weft yarn by twisting around it, resulting in nearly twice the tensile strength and strain of the FL in the warp direction compared to plain structures of the same density. Moreover, due to the self-locked interweaving of warp yarns, the FL exhibits greater displacement to reach the junction rupture force point in the yarn pull out tests compared to plain structure with the same density. Additionally, the four-warp leno woven fabric demonstrates good air permeability, thermal conductivity, and water vapor transmission due to its high porosity. Consequently, the development of the four-warp leno woven structure provides a novel design approach for functional textiles, medical products, and industrial materials.

Experimental section

Materials and preparation of the fabrics

Cotton yarns with a yarn count of 10/3S were provided by the laboratory. The four-warp leno woven fabric was fabricated using advanced weaving techniques. Firstly, the improved needle-shaped heald frames were constructed. The first and second needle-shaped heald frames were employed as leno heald frames (for doup yarns), while the third and fourth frames served as base heald frames (for ground yarns). Secondly, four warp yarns were grouped together, and a skip threading program was utilized to insert the yarns into the frame: the first warp yarn passed through the first frame, the second warp yarn through the third frame, the third warp yarn through the second frame, and the fourth warp yarn through the fourth frame. With four warp yarns constituting a group and two groups of eight warp yarns forming the minimum weaving unit, weaving was conducted in cycles of four shuttles.

Characterization and measurements

The surface morphologies of the prepared fabrics were analyzed using the Leica M165C (DFC 290HD, Leica Microsystems Ltd.). Fabric thickness measurements were conducted with the AMES thickness tester (Model BG1110-1–04) in accordance with standard ASTM D1777-96. The specimen was positioned with the face side up on the anvil of the thickness gauge. The presser foot was slowly lowered until it made contact with the specimen, taking 5 to 6 s to apply full pressure on the fabric. The thickness value was recorded, and the test was repeated five times for accuracy.

The tensile strength test was performed to assess the mechanical characteristics of the fabrics according to standard ASTM D5035. During this test, a tensile force was applied to the fabric specimen until it ruptured. The Instron 5566 was used to evaluate the fabric's breaking strength and strain at a temperature of 20 ± 2 °C and a relative humidity of 65 ± 4%. The specimen size was approximately 200 × 50 mm, with a stretching velocity of 300 mm/min and a gauge length of 75 mm. Three repeated measurements were conducted in both the warp and weft directions for each fabric.

The Instron 5566 was utilized to conduct the single yarn pull-out test. In this test, the upper grip clamped the top of a single yarn positioned at the center of the fabric, while the lower fixed grip held the bottom part of the fabric. The upper grip ascended at a velocity of 100 mm/min until the single yarn was fully extracted from the fabric. The gauge length was set at 100 mm, and the testing temperature and humidity were maintained at 20 °C and 65%, respectively. The samples were prepared with dimensions of 150 mm × 35 mm, and the tests were repeated three times.

The KES-FB-2 bending tester was employed to evaluate the bending performance of the fabrics (Süle 2012). The KES system operates on the principle of pure bending, where the fabric specimen is bent into an arc of continuously varying curvature. The specimen width in the KES setup was 200 mm. The bending test involved cyclically flexing a fabric sample back and forth between two fixed points, generating a bending curve that correlates the bending moment (M) with the fabric's curvature (K). Bending rigidity (B) and bending hysteresis (2HB) were determined from the obtained bending curve.

To accurately measure the air permeability of the fabrics, an air permeability tester (KES-F8, Kato Tech Co., Ltd.) was used (Chen et al. 2015). The evaluated performance index was air flow resistance (R), with higher air resistance indicating lower permeability. The specimen dimensions were 100 × 100 mm, and the test was repeated three times.

Additionally, the thermal conductivity of the fabric was examined using the KES-F7 Thermo Labo II Instrument, as shown in Fig. 1. First, room temperature water was circulated in the "water box," and the water box temperature was set to 25 °C, while the temperature of the BT-Box was set to 35 °C. Next, the sample was placed on the "water box." Once the temperatures of the "BT-Box" and the guard reached the pre-set levels, the "BT-Box" was positioned on the sample to ensure complete contact between the BT plate and the sample. Finally, the "W" button was

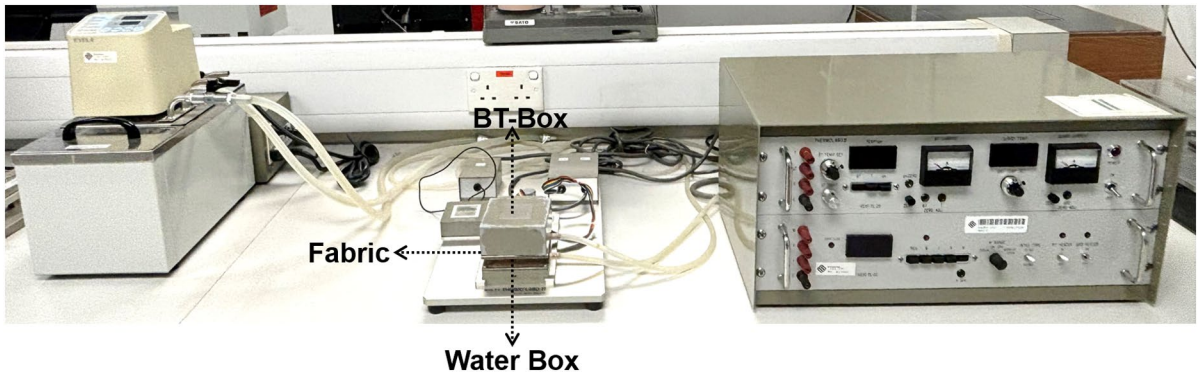

Fig. 1 Thermal conductivity testing equipment of fabric

pressed, and once the readings stabilized, the value displayed on the digital panel was recorded. In this test, the weight of the "BT-Box" was 150 g, resulting in a pressure of 6 gf/cm^2 during measurement. The test was repeated five times. The thermal conductivity of the fabric is calculated using the following Eq. (1):

$$k = \frac{W \times D}{A \times \Delta T_0} \tag{1}$$

where W denotes the heat consumption in watts. D represents the sample thickness in cm, A indicates the area of the BT-Box in cm^2. Additionally, ΔT_0 refers to the temperature difference of BT-box and water box in °C. The area A was standardized at 25 cm^2, and ΔT_0 was established at 10 °C.

The water vapor transmission of the fabric was measured according to GB/T 12704.1–2009 Part 1: Desiccant method. Each test was repeated three times. The testing conditions were set at a temperature of 38 °C and a relative humidity of 90%. The fabric samples were placed within a moisture-permeable cup filled with desiccant calcium chloride. After a specified time interval, the mass change of the moisture-permeable cup was recorded, allowing for the calculation of water vapor transmission using Eq. (2):

$$WVT = \frac{24\Delta m_c}{St} \tag{2}$$

where WVT represents the water vapor transmission measured in grams per square meter per day (g/m^2/24 h); Δm_c indicates the difference in weight between two consecutive measurements of the same test combination, measured in grams (g); S denotes the effective test area of the sample, measured in square meters (m^2); and t signifies the duration of the test, measured in hours (h).

Results and discussion

Design and fabrication of a four-warp leno fabric

To conduct this study, fabrics with high breathability and mechanical properties were prepared based on four criteria: (i) designing the fabric structure with high porosity to allow airflow between the body and the external environment, (ii) creating more yarn intersection points to increase friction between yarns and enhance the pulling force, (iii) enhancing the curvature of the yarns in the fabric structure to improve their displacement during pulling, and (iv) constructing a higher interweaving angle to strengthen the frictional force. To satisfy these requirements, a four-warp leno weave structure was designed (Fig. 2a). As shown in Fig. 2b, cotton yarns were selected for fabricating the leno fabrics due to their inherent breathability, good moisture absorption, and softness. Subsequently, modified weaving technology was employed to fabricate the fabrics using needle-shaped heald frames. Figure 2c presents a photo and optical microscope image of the fabricated four-warp leno fabric. It can be observed that the four-warp leno structure consists of four warp yarns as a group, including ground yarns and doup yarns, resulting in a flat mesh structure. There is no interlacement between the ground yarns and the weft yarns; the ground yarns are always positioned below the weft yarns and are only interlaced with the doup yarns.

Characterization of fabric structure

To compare the structural effects, four types of fabrics with different structures were designed and fabricated: a high-density plain fabric, and plain, leno, and four-warp leno fabrics with the same density. The plain and leno fabrics were produced using conventional weaving technology. The high-density plain structure (HP) served as the reference, with a warp density of 11 threads/cm and a weft density of 9 threads/cm. In contrast, the plain (LP), leno (TL), and four-warp leno (FL) structures were developed with a warp density of 11 threads/cm and a weft density of 4 threads/cm for comparison. The surface morphologies of the developed fabrics were observed using optical microscopy. From Fig. 3a and b, it can be seen that the plain fabrics with high and low densities create tight, regular grid-like structures. Figure 3c illustrates the leno fabric structure, which comprises two warp yarn systems, including straight and leno yarns, intertwining with each other and the inserted weft yarn. In contrast to a plain weave, a leno weave involves twisting the warp yarns into a series of “8” shapes and inserting the weft yarns into the gaps, resulting in a sturdy and breathable weave. Compared to the plain and leno structures, the four warp threads cross each other and interlock with the weft yarn by twisting around it, as shown in Fig. 3d. Figure 3e and

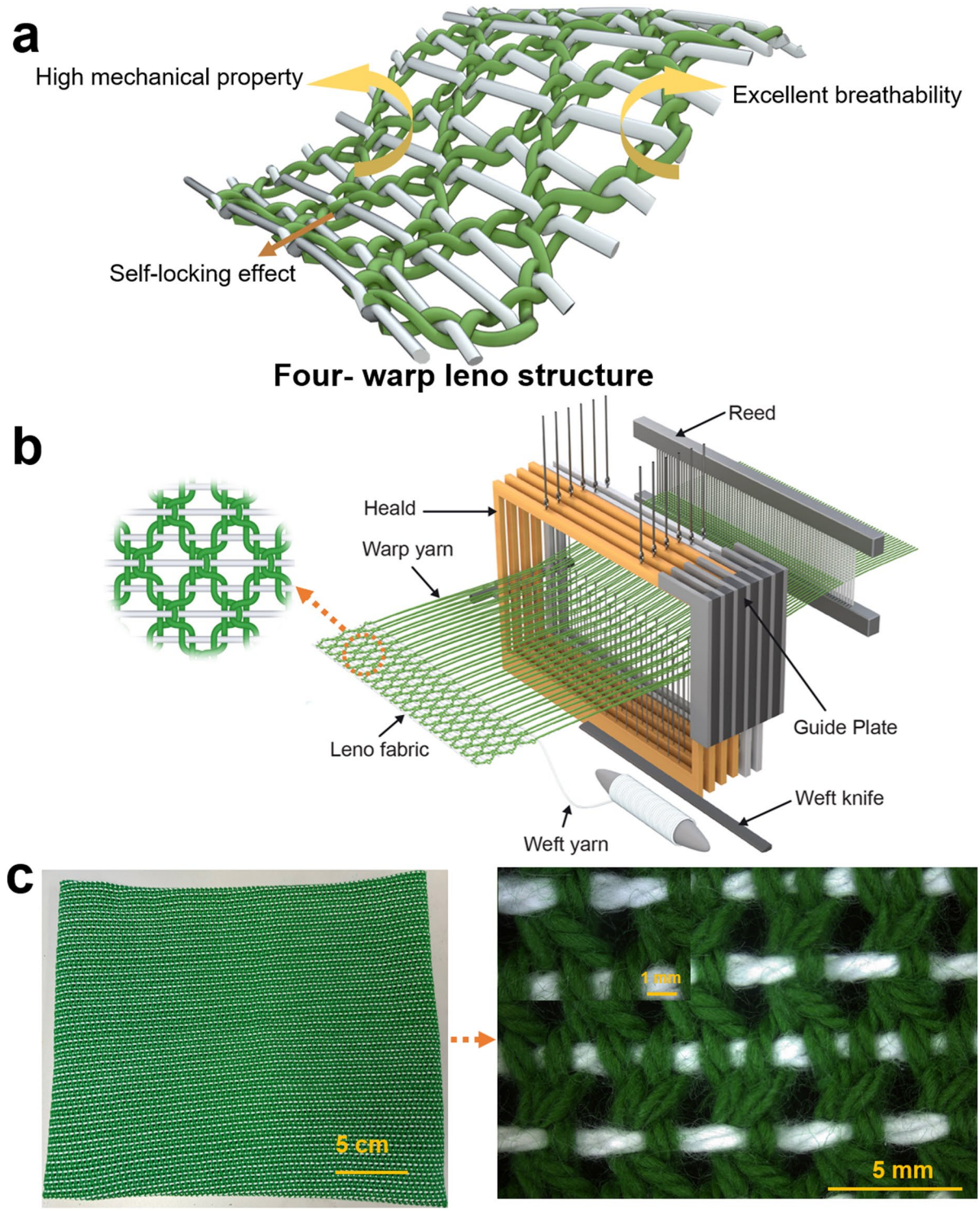

Fig. 2 Structural design and manufacturing of the fabric. **a** Structural design of the four-warp leno weave. **b** Weave process of the four-warp leno weave. **c** Photo and optical microscope image of the fabricated four-warp leno fabric

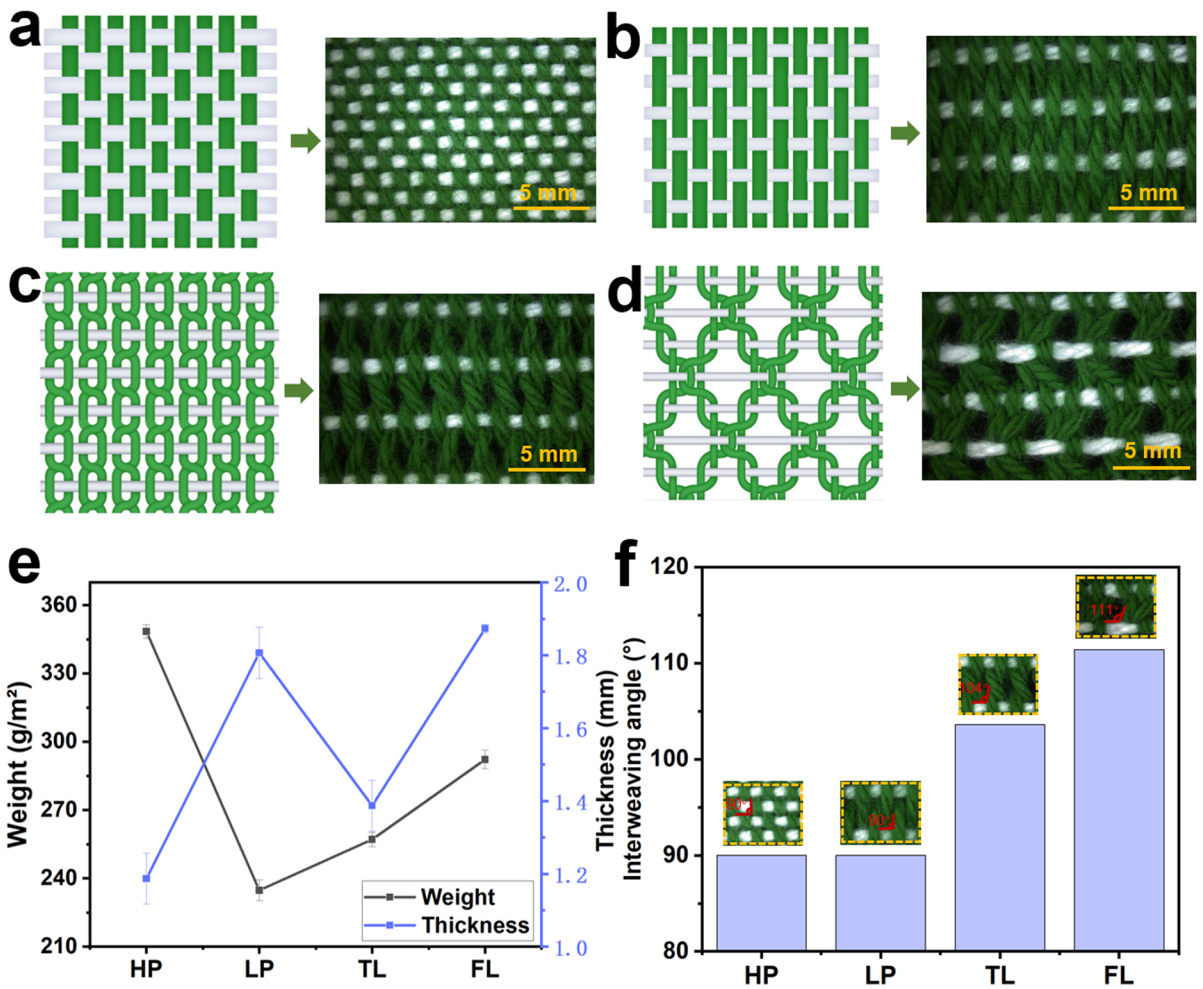

Fig. 3 Characterization of the FL. Schematic diagrams and optical microscope images of the fabrics with **a** plain structure in high density, **b** plain structure in low density, **c** leno structure and **d** four-warp leno structure. **e** Fabric weight and thickness of the four fabrics. **f** Interweaving angles of warp and weft yarns in the four fabric structures

f present the specifications of the four fabrics, including weight, thickness, and the interweaving angle between the weft and warp yarns. From Fig. 3e, it is evident that the four-warp leno woven fabric has a higher weight, approximately 287.8 g/m^2, compared to the plain and leno fabrics with the same density. Among the four fabrics, the high-density plain fabric shows the lowest thickness, while the four-warp leno weave presents the highest thickness, measuring about 1.8 mm. Additionally, the thickness of LP is comparable to that of FL. The thickness of a fabric is influenced not only by its weight but also by its structure, including factors such as the arrangement and interlacing of the yarns. In low-density plain weave fabric, the yarns are minimally compressed, maintaining their original cylindrical shape. In contrast, in a four-warp leno weave, the yarns are pressed against one another, resulting in a flattened appearance. Therefore, although LP is lighter, its thickness is similar to that of FL. The interweaving angle of the warp and weft yarns is also an important structural parameter that impacts fabric properties. As shown in Fig. 3f, the plain structure, leno structure, and four-warp leno structure present interweaving angles of 90°, 104°, and 111°, respectively. Due to its unique structural characteristics, the four-warp leno weave exhibits the largest interweaving angle.

Tensile properties

The tensile strength of a fabric is a crucial performance metric that determines its ability to withstand pulling or stretching forces without breaking or tearing. This is important in various applications, such as clothing, apparel, and industrial and technical uses. The tensile strengths of the fabrics in the warp and weft directions are depicted in Fig. 4. As shown in Fig. 4a and b, the resultant fabric FL, featuring a four-warp leno structure, exhibits the highest breaking load (1006 N) and strain (40%) in the warp direction compared to LP and TL, which have the same density, as well as HP, which has a higher density. The breaking strength and strain of FL are nearly twice that of a plain weave with the same density. This superior performance can be attributed to the fact that FL demonstrates the highest self-locking effect between the warp yarns. The intertwining of the four warp yarns increases friction between them, providing greater resistance to forces in the warp direction during tensile strength testing. It is also noteworthy that FL possesses the highest strain along the warp direction, measuring about 40%. The intertwining of the warp yarns in the FL structure increases the buckling length of the yarns, resulting in greater strain in the warp direction when compared with other weaving structures. Figure 4b illustrates the breaking curve of the four fabrics along the warp direction, detailing the breaking process. The tensile fracture curves of the four fabric types are similar and can be divided into four main stages. The first stage involves the

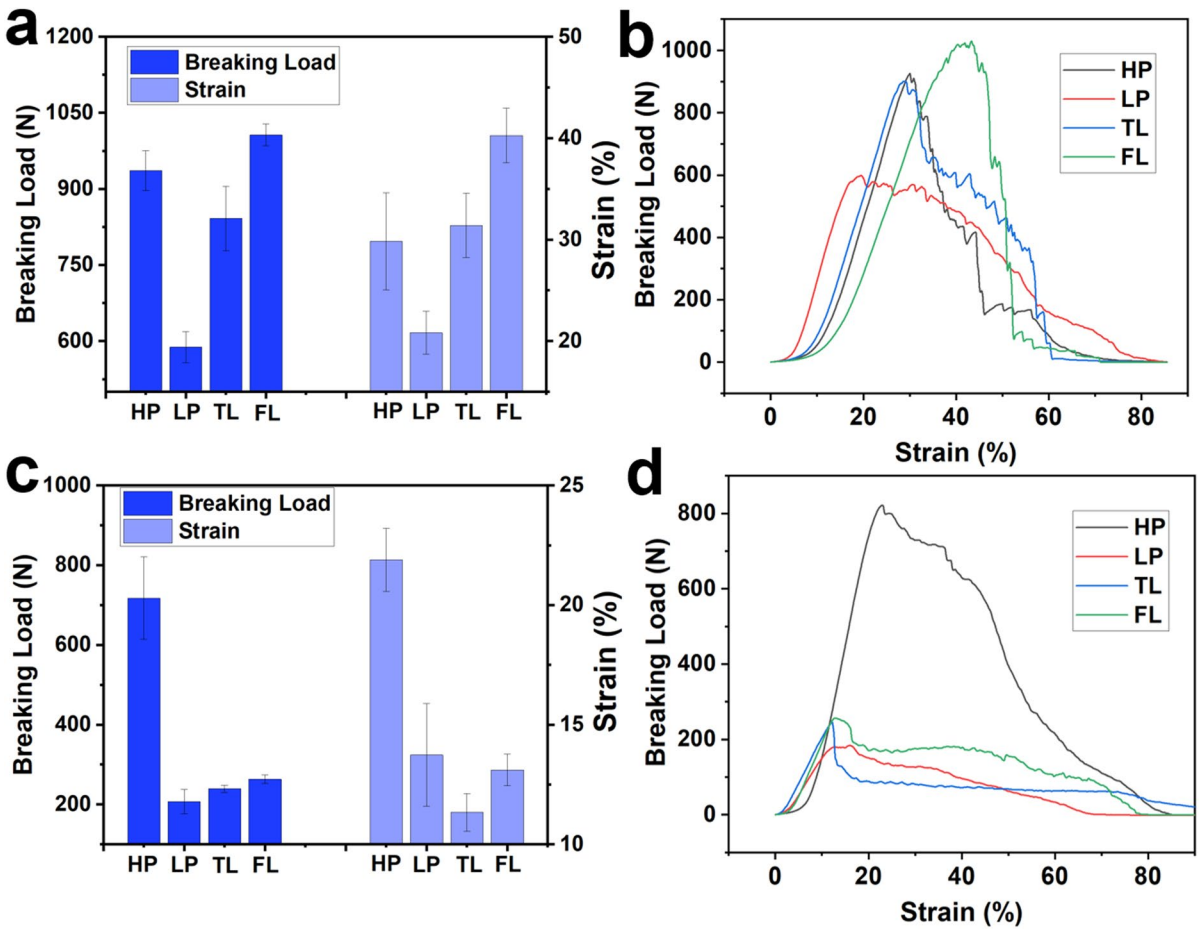

Fig. 4 Tensile property of the FL. **a** Comparison of the tensile properties of different fabrics along the warp direction. **b** Tensile curves of four woven fabrics along the warp direction. **c** Comparison of the tensile properties of different fabrics along the weft direction. **d** Tensile curves of four woven fabrics along the weft direction

straightening of the warp yarns under tension. In the second stage, elastic deformation occurs, where the straightened yarns begin to bear more stress. The third stage features the asynchronous fracture of fibers and yarns, leading to a decrease in the slope of the tensile curve compared to the second stage. Finally, most of the yarns fracture, some slip, and the fabric ultimately fails.

Figure 4c presents the tensile strength of the fabric in the weft direction. The results indicate that HP, with a higher weft density, exhibits the highest breaking load and strain. As the fabric density increases, the number of load-bearing yarns per unit area also increases. This higher yarn density results in more contact points between the yarns, improving yarn-to-yarn friction and load distribution. However, FL consistently demonstrates better breaking load and strain compared to the plain and leno fabrics with the same density, which can also be attributed to the locking effect between the warp yarns. The breaking curves of the four fabrics are presented in Fig. 4d. Compared to the plain weave structure, the fabric with a leno structure exhibits more load fluctuations after breaking.

Yarn pull-out behavior

To understand the structure–property relationship of different woven structures, yarn pull-out behavior is considered the most important method for examining the structural effects of woven fabrics. The single warp yarn pull-out load and displacement results obtained from four different structure-based woven fabrics are presented in Fig. 5a. When a yarn is pulled, the yarn tension reaches a value known as the junction rupture force or peak load force. The testing results show that the warp yarn within the plain woven fabric with higher density requires the maximum load (8 N) to reach the junction rupture force point compared to all other developed woven fabrics. It is also noted that the warp yarn of the plain woven fabric with higher density exhibits an excellent gripping effect, resulting in almost 16 mm of displacement. Among the woven fabrics with the same density, the plain woven fabric with lower density requires the minimum load to reach the junction rupture force point. In contrast, the TL with a leno structure and FL with a four-warp leno structure require a higher load to reach this point compared to the plain fabric with the same density. However, significant variations are observed among the fabrics of the same density when considering yarn displacement. The leno fabric and four-warp leno fabric demonstrate greater displacements of 21–23 mm, respectively. The plain woven fabric with lower density begins displacing (with a yarn displacement of 8 mm) shortly after the test starts. These unusual results can be attributed to the structural differences of the developed woven fabrics. Figure 5b presents the load–displacement curves for the single warp yarn pull-out of the four fabrics. It can be observed that the pull-out force for all four fabrics drops rapidly after reaching the peak load force. Compared to the plain weave structure, the pull-out forces of TL and FL fluctuate repeatedly due to the self-locking effect between the warp yarns in the weave structure.

For the pull-out of the weft yarn, the results show that the plain fabric structure with higher density exhibits the highest peak load force and displacement among the four different fabric structure configurations (Fig. 5c). However, the peak load force (2 N) and displacement (8 mm) of the FL fabric are greater than those of LP (0.4 N and 5 mm) and TL (1 N and 6 mm) with the same density during the pulling of a single weft yarn. The corresponding pull-out curves are shown in Fig. 5d, indicating the changes in displacement and force during the pulling of a single weft yarn. These curves can be explained using two distinct regions: the static friction region and the kinetic friction region for all developed fabrics.

Figures 5e and f show the detailed pull-out curves for the four-warp leno structure when pulling the warp yarn and weft yarn, respectively. Figure 5g further illustrates the fabric behavior during the yarn pull-out. During the static region, the extracted yarn experiences crimp extension and produces static friction at the intersection points, leading to fabric deformation or lifting from the bottom side. Consequently, the yarn pull-out load reaches the junction rupture force point, after which the pulled yarn begins to slip, marking the transition into the kinetic friction region. Within this region, the curve exhibits a wave-like feature related to yarn crimp exchange. The pull-out load initially increases and then decreases. The rise in pull-out force indicates that the lower end of the extracted warp yarn is sliding into the neighboring intersection, while the decline in force suggests that it is slipping out of the current intersection. The pulled yarn load continuously decreases until the yarn is

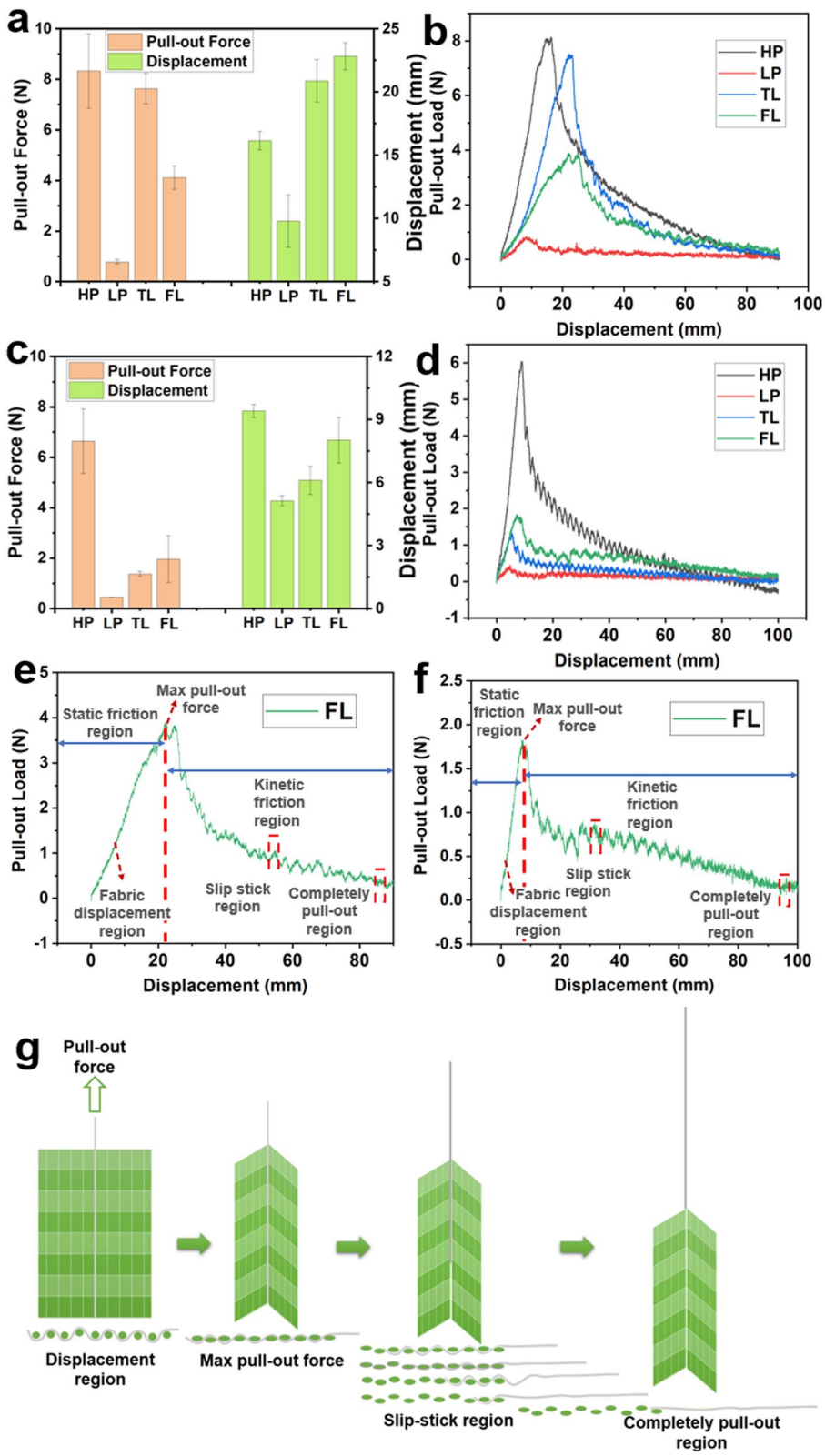

Fig. 5 Yarn pull-out property of the FL. **a** Comparison of the pull-out property of warp yarn within four woven fabrics. **b** Pull-out curves of warp yarn within four woven fabrics. **c** Comparison of the pull-out property of weft yarn within four woven fabrics. **d** Pull-out curves of weft yarn within four woven fabrics. Pull-out force versus displacement of **e** the warp and **f** weft yarn of the FL. **g** Schematic diagram of the single yarn pull-out process

fully extracted. Thus, the curve reflects the deformation of the fabric and yarn, illustrating the processes of yarn crimp extension, crimp exchange, and friction slip.

Fabric bending behavior

Fabric bending rigidity is a crucial factor influencing garment flexibility and comfort. The bending hysteresis of a fabric significantly impacts its dimensional stability, pleat durability, wrinkle recovery, and overall drape. Fabrics with low bending hysteresis return to their original shape more quickly, offering a softer and more comfortable feel against the skin. Moreover, a fabric's bending characteristics affect how it hangs and flows, allowing for an ideal aesthetic in clothing and interior design. In applications such as activewear and outdoor gear, fabrics must endure repeated bending without compromising their integrity and must be able to recover to their original state. Low bending hysteresis enhances performance under dynamic conditions. Therefore, evaluating a fabric's bending behavior is essential. Figure 6 illustrates the flexibility-related bending behavior of the fabrics, with bending rigidity (B) and bending hysteresis (2HB) serving as two evaluation metrics. Bending rigidity represents the slope of the linear portion of the bending curve and indicates the fabric's resistance to bending; a lower B value signifies higher bending ease. Bending hysteresis measures the difference of moment

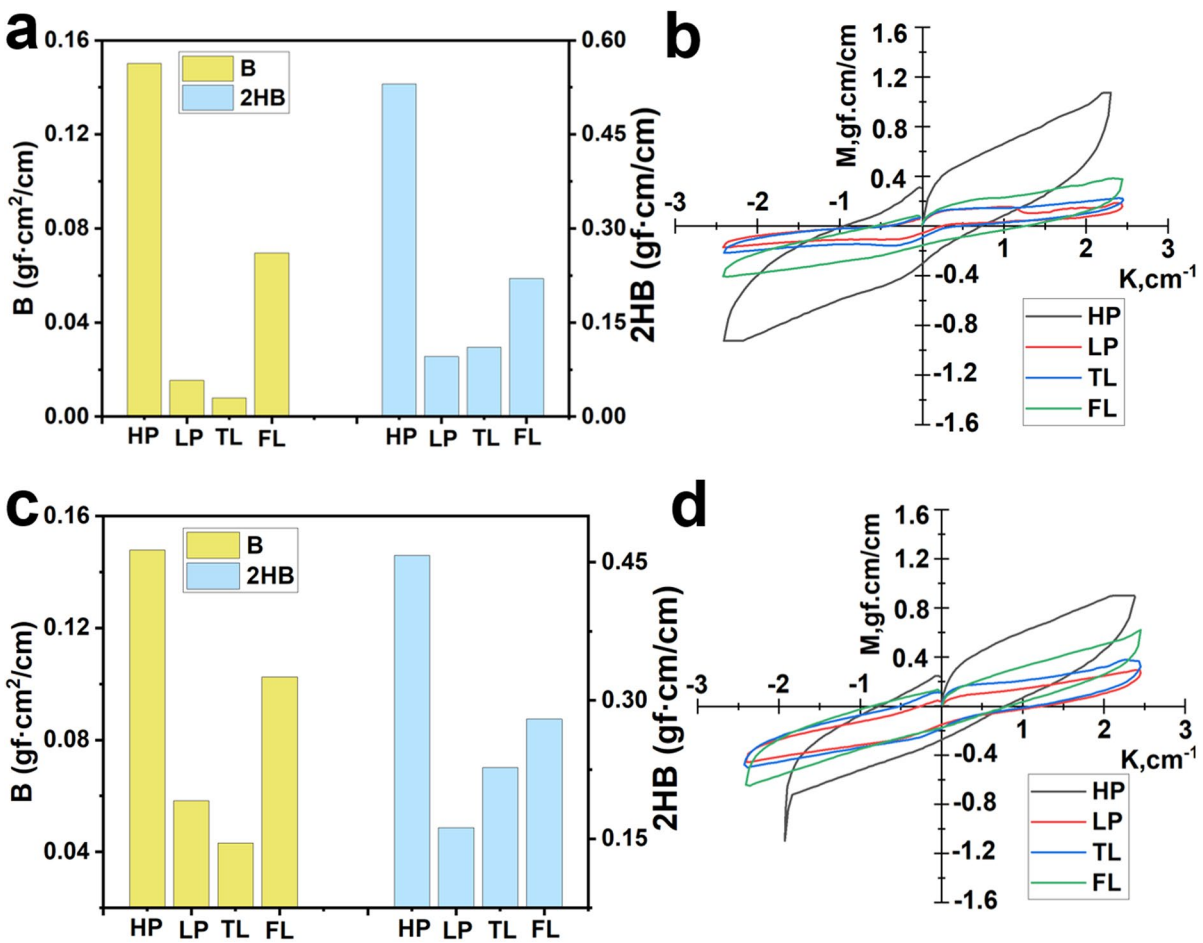

Fig. 6 Bending behavior of the FL. **a** Comparison of the bending properties of four woven fabrics along the warp direction. **b** Bending curves of four woven fabrics along the warp direction. **c** Comparison of the bending properties of four woven fabrics along the weft direction. **d** Bending curves of four woven fabrics along the weft direction

between the loading and unloading portions at the 1/cm curvature of the bending curve, with a lower 2HB value indicating better bending recovery.

Figure 6a and b show the bending properties of the fabrics in the warp direction. The results indicate that the plain fabric with higher density (HP) possesses the highest bending rigidity and bending hysteresis among the four fabrics, reflecting the lowest flexibility. Additionally, the fabric with the four-warp leno structure exhibits higher bending rigidity (0.0696 gf·cm^2/cm) and bending hysteresis (0.2202 gf·cm/cm) compared to the LP and TL fabrics of the same density, illustrating lower bending ease and bending recovery. This can be attributed to the self-locking effect between the warp yarns, which limits the bending of the four-warp leno fabric. Furthermore, the trend in the bending test results for the fabrics in the weft direction is consistent with that in the warp direction, as shown in Fig. 6c and d.

Breathability

As we all know, breathability is one of the most crucial properties of protective clothing, significantly influencing wearing comfort. As shown in Fig. 7a, the developed four-warp leno fabric exhibits superior air permeability (low air resistance) compared to the higher air resistance of plain and leno fabrics. Furthermore, the FL fabric also demonstrates better thermal conductivity when compared with the plain fabric of the same density. To identify significant differences in air permeability and thermal conductivity, the data were analyzed using one-way analysis of variance (ANOVA) with IBM SPSS Statistics software. A p-value of less than 0.05 indicates statistical significance. The ANOVA results revealed significant differences in air permeability among LP, TL, and FL ($p<0.01$). Similarly, significant differences were observed in the thermal conductivity of these fabrics ($p=0.007$). Following this, Least Significant Difference (LSD) tests were conducted for multiple comparisons of fabric air permeability and thermal conductivity, with the results summarized in Table 1. Significant differences in air permeability were noted across fabric samples with different structures. Additionally, the thermal conductivity of the fabrics also showed significant differences, except for the pair of fabric samples LP and FL. The measured results

Table 1 LSD test results of multiple comparisons of fabric air permeability and thermal conductivity

Fabric		Air permeability		Thermal conductivity	
		Mean difference	Sig	Mean difference	Sig
LP	TL	0.020*	0.001	–0.006*	0.003
	FL	0.030*	< 0.001	–0.003	0.064
TL	LP	-0.020*	0.001	0.006*	0.003
	FL	0.010*	0.032	0.003*	0.036
FL	LP	-0.030*	< 0.001	0.003	0.064
	TL	-0.010*	0.032	–0.003*	0.036

*The mean difference is significant at the 0.05 level

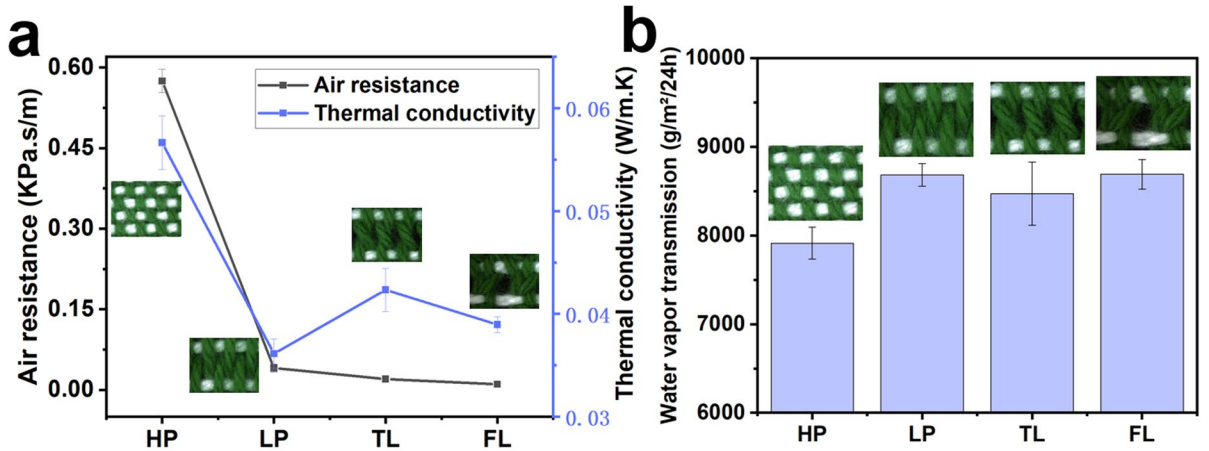

Fig. 7 Breathable properties of the FL. **a** Air permeability and thermal conductivity of the four fabrics. **b** Water vapor transmission of the four fabrics

Table 2 LSD test results of multiple comparisons of fabric water vapor transmission

Fabric		Water vapor transmission	
		Mean difference	Sig
LP	HP	770.000*	0.003
	TL	213.333	0.278
	FL	–6.667	0.972
TL	HP	556.667*	0.016
	LP	–213.333	0.278
	FL	–220.000	0.264
FL	HP	776.667*	0.003
	LP	6.667	0.972
	TL	220.000	0.264
HP	LP	–770.000*	0.003
	TL	–556.667*	0.016
	FL	–776.667*	0.003

*The mean difference is significant at the 0.05 level

indicate that the four-warp leno structure is suitable for wearing.

Furthermore, the water vapor transmission of the resulting four-warp leno fabric was investigated, as it is another crucial aspect influencing breathability and comfort. As shown in Fig. 7b, the water vapor transmission of the fabricated FL fabric is as high as 8690 g/m^2/24 h, due to the large spacing between the interlaced yarns. As expected, the plain fabric with higher density exhibits a much lower water vapor transmission of 7913 g/m^2/24 h, primarily because of its decreased porosity. The water vapor transmission of HP, LP, TL, and FL was also analyzed using ANOVA. The results indicated that the water vapor transmission of these fabrics shows significant differences ($p = 0.009$). The LSD tests for multiple comparisons of fabric water vapor transmission demonstrate that HP exhibits significant differences when compared to LP, TL, and FL, respectively (see Table 2).

Conclusions

In summary, a programmed mesh-like four-warp leno fabric with outstanding mechanical performance and breathability has been developed using improved needle-shaped heald frames for diverse applications. The strategy of utilizing self-locking effects by manipulating the interweaving of the warp yarns to simultaneously regulate yarn friction and fabric porosity enhances tensile strength, pull-out displacement, and breathability. Specifically, compared to the plain structure with equivalent density, FL exhibits approximately double the tensile strength and strain in the warp direction. Additionally, the four-warp leno fabric demonstrates greater displacements to reach the junction rupture force point than the plain structure with the same density in the yarn pull out tests, owing to the self-interlocking weaving of the warp yarns. Furthermore, the four-warp leno fabric possesses the lowest air resistance among the four fabrics, measuring about 0.01 kPa·s/m, along with high water vapor transmission (8690 g/m^2/24 h). These mechanical performance and breathability characteristics position the four-warp leno fabric as a promising solution for various application scenarios.

Acknowledgements The authors wish to thank the Hong Kong General Research Fund for funding support the project (Project No. 15607920).

Author contributions All authors contributed to the experiments of this study and approved the final manuscript. Tian. X. wrote the main manuscript text. Li. L. provided the idea and supervised this work.

Funding Open access funding provided by Hong Kong University of Science and Technology. This work was financially supported by the Hong Kong General Research Fund (Project No. 15607920).

Data availability No datasets were generated or analysed during the current study.

Declarations

Conflict of interest The authors declare no competing interests.

Ethical approval Not applicable.

References

Bhattacharjee S, Joshi R, Chughtai AA, Macintyre CR (2019) Graphene modified multifunctional personal protective clothing. Adv Mater Interfaces 6:1900622

Cai WH, Li TT, Zhang XX (2023) Polyacrylate and carboxylic multi-walled carbon nanotube-strengthened aramid fabrics as flexible puncture-resistant composites for anti-stabbing applications. ACS Appl Nano Mater 6:6334–6344

Chen Q, Fan J, Sun C (2015) The comfort evaluation of weft knitted plant structured fabrics and garment. I. objective evaluation of weft knitted plant structured fabrics. Fibers Polym 16:1788–1795

Gong X, Xu Y, Zhu W, Xuan S, Jiang W, Jiang W (2014) Study of the knife stab and puncture-resistant performance for shear thickening fluid enhanced fabric. J Compos Mater 48:641–657

Houshyar S, Padhye R, Nayak R (2017) Effect of moisture-wicking materials on the physical and thermo-physiological comfort properties of firefighters' protective clothing. Fibers Polym 18:383–389

Iftikhar F, Hussain T, Ali Z, Nazir A, Adolphe DC, Schacher L (2020) Investigation of thermo-physiological comfort and mechanical properties of fine cotton fabrics for ladies' summer apparel. J Nat Fibers 17:1619–1629

Jahan I (2017) Effect of fabric structure on the mechanical properties of woven fabrics. Adv Res Text Eng 2:1018

Kalazić A, Brnada S, Kiš A (2022) Thermal protective properties and breathability of multilayer protective woven fabrics for wildland firefighting. Polymers 14:2967

Lenz C, Schröter A, Johnen C, Gloy YS, Gries T (2015) New production technology for multiple leno fabrics based on propeller lenos. Melliand Int.

Lepage ML, Takaffoli M, Simhadri C, Mandau R, Gashti MP, Nazir R, Mohseni M, Li W, Liu C, Bi L, Falck G, Berrang P, Golovin K, Milani AS, DiLabio GA, Wulff JE (2021) Influence of topical cross-linking on mechanical and ballistic performance of a woven ultra-high-molecular-weight polyethylene fabric used in soft body armor. ACS Appl Polym Mater 3:6008–6018

Limeneh DY, Ayele M, Tesfaye T, Liyew EZ, Tesema AF (2022) Effect of weave structure on comfort property of fabric. J Nat Fibers 19:4148–4155

Nasser J, Steinke K, Groo L, Sodano HA (2019) Improved interyarn friction, impact response, and stab resistance of surface fibrilized aramid fabric. Adv Mater Interfaces 6:1900881

Pamuk G, Cüreklibatır Encan B, Yıldız EZ (2023) Thermal Characteristics, Mechanical and Comfort Properties of Heat-Protective Textiles. Fibers Polym 24:4457–4468

Qiu Y, Wu L, Liu S, Yu W (2023) Impact-protective bicontinuous hydrogel/ultrahigh-molecular weight polyethylene fabric composite with multiscale energy dissipation structures for soft body armor. ACS Appl Mater Interfaces 15:10053–10063

Saha J, Rahman M, Kabir MR, Emtiaz ANM, Islam MR, Jafor A (2017) Study on manufacturing process of leno weave by modification of hand loom. J Sci Technol 7:157–170

Sanchez V, Walsh CJ, Wood RJ (2021) Textile technology for soft robotic and autonomous garments. Adv Funct Mater 31:2008278

Schwarz I, Kovačević S, Vitlov I (2020) Influential parameters of starching process on mechanical properties of yarns intended for multifunctional woven fabrics for thermal protective clothing. Polymers 13:73

Shaker K, Nawab Y, Ayub Asghar M, Nasreen A, Jabbar M (2020) Tailoring the properties of leno woven fabrics by varying the structure. Mech Adv Mater Struct 27:1865–1872

Süle G (2012) Investigation of bending and drape properties of woven fabrics and the effects of fabric constructional parameters and warp tension on these properties. Text Res J 82:810–819

Tan Y, Ma Y, Liu J, Liu Z, Wu F, Li Y (2024) Breathable and impact-resistant shear thickening gel based three-dimensional woven fabric composites constructed by an efficient weaving strategy for wearable protective equipment. Compos A 177:107886

Tang KPM, Kan CW, Fan JT, Tso SL (2017) Effect of softener and wetting agent on improving the flammability, comfort, and mechanical properties of flame-retardant finished cotton fabric. Cellulose 24:2619–2634

Weise D, Vorhof M, Brünler R, Sennewald C, Hoffmann G, Cherif C (2019) Reduction of weaving process-induced warp yarn damage and crimp of leno scrims based on coarse high-performance fibers. Text Res J 89:3326–3341

Yi Z, Ali M, Gong X, Dai H, Zhongmin D (2019) An experimental investigation of the yarn pull-out behavior of plain weave with leno and knitted insertions. Text Res J 89:4717–4731

Zhang X, Wang X, Peng Z, Zhu Z, Wu Z (2020) Parametric study on mechanical properties of basalt leno textile applied as concrete reinforcement. Adv Struct Eng 25:48–62

Zhao K, Cao S, Xu G (2023) An experimental study of mechanical properties and comfortability of knitted imitation woven shirt fabrics. Autex Res J 24:20230001

Zhou Y, Chen X, Wells G (2014) Influence of yarn gripping on the ballistic performance of woven fabrics from ultra-high molecular weight polyethylene fibre. Compos B 62:198–204